Magnetometry with a nanometric-thin K vapor cell

R. Momier[1,2,*], A. Sargsyan[2], A. Tonoyan[2], M. Auzinsh[3], D. Sarkisyan[2], A. Papoyan[2] and C. Leroy[1]

[1]Laboratoire ICB, UMR CNRS 6303, Université Bourgogne Franche-Comté, 21000 Dijon, France
[2]Institute for Physical Research, NAS of Armenia, Ashtarak-2, 0203 Armenia
[3]Department of Physics, University of Latvia, Rainis boulevard 19, LV-1586, Riga, Latvia
[*]rodolphe.momier@u-bourgogne.fr

International Conference - **L**aser **P**hysics 2022 (LP-2022)

Table of Contents

Table of Contents

Theory - Magnetic Hamiltonian

The magnetic Hamiltonian (from Dirac equation) reads

$$H_m = \frac{e}{2m_e c}(\mathbf{p} \cdot \mathbf{A} + \mathbf{A} \cdot \mathbf{p}) + \frac{e}{m_e c}\mathbf{S} \cdot \nabla \times \mathbf{A}$$

Theory - Magnetic Hamiltonian

The magnetic Hamiltonian (from Dirac equation) reads

$$H_m = \frac{e}{2m_e c}\left(\mathbf{p}\cdot\mathbf{A} + \mathbf{A}\cdot\mathbf{p}\right) + \frac{e}{m_e c}\mathbf{S}\cdot\nabla\times\mathbf{A} = \boxed{\frac{\mu_B}{\hbar}\mathbf{B}\cdot\left(\mathbf{L}+2\mathbf{S}\right)}.$$

Remark

This is valid in the case of a static magnetic field such that

$$\mathbf{A} = \frac{1}{2}\left(\mathbf{B}\times\mathbf{r}\right).$$

Theory - Magnetic Hamiltonian

Including the nuclear spin yields

$$\mathcal{H}_m = \frac{\mu_B}{\hbar} B_z (g_L L_z + g_S S_z + g_I I_z)\,.$$

P. Tremblay et al. "Absorption profiles of alkali-metal D lines in the presence of a static magnetic field". *Phys. Rev. A* **42** (1990), p. 2766.

Theory - Magnetic Hamiltonian

Including the nuclear spin yields

$$\mathcal{H}_m = \frac{\mu_B}{\hbar} B_z (g_L L_z + g_S S_z + g_I I_z) \,.$$

The matrix elements of $\mathcal{H}$ are:

$$\langle F, m_F | \, \mathcal{H} \, | F, m_F \rangle = E_0(F) - \mu_B g_F m_F B_z$$

P. Tremblay et al. "Absorption profiles of alkali-metal D lines in the presence of a static magnetic field". *Phys. Rev. A* **42** (1990), p. 2766.

Theory - Magnetic Hamiltonian

Including the nuclear spin yields

$$\mathcal{H}_m = \frac{\mu_B}{\hbar} B_z (g_L L_z + g_S S_z + g_I I_z)\,.$$

The matrix elements of $\mathcal{H}$ are:

$$\langle F, m_F | \, \mathcal{H} \, | F, m_F \rangle = E_0(F) - \mu_B g_F m_F B_z$$

$$\langle F-1, m_F | \, \mathcal{H} \, | F, m_F \rangle = -\frac{\mu_B}{2}(g_J - g_I) B_z \left(\frac{[(J+I+1)^2 - F^2][F^2 - (J-I)^2]}{F} \right)^{1/2} \times \left(\frac{F^2 - m_F^2}{F(2F+1)(2F-1)} \right)^{1/2} .$$

With $|J - I| \leq F \leq J + I$ and $-F \leq m_F \leq F$.

P. Tremblay et al. "Absorption profiles of alkali-metal D lines in the presence of a static magnetic field". *Phys. Rev. A* **42** (1990), p. 2766.

Theory - Magnetic Hamiltonian

Remark

The Hamiltonian is m_F-block diagonal. The off-diagonal elements obey $\Delta F = \pm 1$, $\Delta m_F = 0$.

A. Aleksanyan et al. "Transition cancellations of ^{87}Rb and ^{85}Rb atoms in magnetic field". *J. Opt. Soc. Am. B* **37** (2020), pp. 3504–3514.

Theory - Magnetic Hamiltonian

Remark

The Hamiltonian is m_F-block diagonal. The off-diagonal elements obey $\Delta F = \pm 1$, $\Delta m_F = 0$.

$$H_g =$$

$$\begin{array}{c}
|F_g=2, m_g=-2\rangle \; |F_g=2, m_g=-1\rangle \; |F_g=1, m_g=-1\rangle \; |F_g=2, m_g=0\rangle \; |F_g=1, m_g=0\rangle \; |F_g=2, m_g=1\rangle \; |F_g=1, m_g=1\rangle \; |F_g=2, m_g=2\rangle \\
\begin{pmatrix}
\zeta + 2\mu_B B g_g & 0 & 0 & 0 & 0 & 0 & 0 & 0 \\
0 & \zeta + \mu_B B g_g & \sqrt{3}\mu_B B(g_I - g_g) & 0 & 0 & 0 & 0 & 0 \\
0 & \sqrt{3}\mu_B B(g_I - g_g) & \mu_B B(2g_I - g_g) & 0 & 0 & 0 & 0 & 0 \\
0 & 0 & 0 & \zeta & 2\mu_B B(g_I - g_g) & 0 & 0 & 0 \\
0 & 0 & 0 & 2\mu_B B(g_I - g_g) & 0 & 0 & 0 & 0 \\
0 & 0 & 0 & 0 & 0 & \zeta - \mu_B B g_g & \sqrt{3}\mu_B B(g_I - g_g) & 0 \\
0 & 0 & 0 & 0 & 0 & \sqrt{3}\mu_B B(g_I - g_g) & \mu_B B(g_g - 2g_I) & 0 \\
0 & 0 & 0 & 0 & 0 & 0 & 0 & \zeta - 2\mu_B B g_g
\end{pmatrix}
\end{array}$$

Figure: Hamiltonian of the ground state of ^{87}Rb. g_g is a condensed notation for a combination of Landé factors.

A. Aleksanyan et al. "Transition cancellations of ^{87}Rb and ^{85}Rb atoms in magnetic field". *J. Opt. Soc. Am. B* **37** (2020), pp. 3504–3514.

Theory - Transfer coefficients

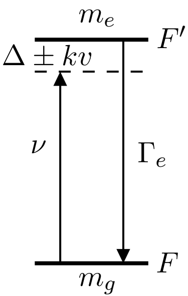

Figure: Two-level system (two Zeeman states) of resonant frequency ν and lifetime $1/\Gamma_e$.

P. Tremblay et al. "Absorption profiles of alkali-metal D lines in the presence of a static magnetic field". *Phys. Rev. A* **42** (1990), p. 2766.

E. De Clercq et al. "Laser diode optically pumped caesium beam". *Journal de Physique (France)* **45**.2 (1984), pp. 239–247.

Theory - Transfer coefficients

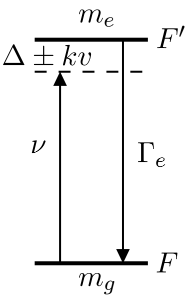

Figure: Two-level system (two Zeeman states) of resonant frequency ν and lifetime $1/\Gamma_e$.

The matrix elements of the electric dipole components are

$$|\langle e| D_q |g\rangle|^2 = \frac{3\epsilon_0 \hbar \lambda^3}{8\pi^2} A_{eg} ,$$

P. Tremblay et al. "Absorption profiles of alkali-metal D lines in the presence of a static magnetic field". *Phys. Rev. A* **42** (1990), p. 2766.

E. De Clercq et al. "Laser diode optically pumped caesium beam". *Journal de Physique (France)* **45**.2 (1984), pp. 239–247.

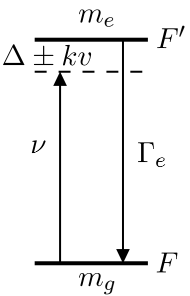

Figure: Two-level system (two Zeeman states) of resonant frequency ν and lifetime $1/\Gamma_e$.

The matrix elements of the electric dipole components are

$$|\langle e| D_q |g\rangle|^2 = \frac{3\epsilon_0 \hbar \lambda^3}{8\pi^2} A_{eg}\,,$$

where the spontaneous emission rate is

$$A_{eg} = \Gamma_e a^2 [\psi(F_e, m_e); \psi(F_g, m_g); q]\,.$$

P. Tremblay et al. "Absorption profiles of alkali-metal D lines in the presence of a static magnetic field". *Phys. Rev. A* **42** (1990), p. 2766.

E. De Clercq et al. "Laser diode optically pumped caesium beam". *Journal de Physique (France)* **45**.2 (1984), pp. 239–247.

Theory - Energy shifts and Transition Probabilities

As an example, we obtain for ^{39}K, D_1 line, σ-polarization:

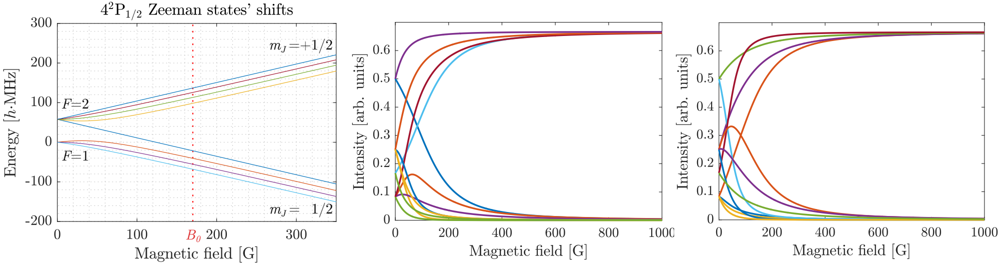

Figure: Left: energy shift of ^{39}K 4^2P$_{1/2}$ Zeeman states. Middle and right: A_{eg}/Γ_e of all possible Zeeman transitions as a function of B for $\sigma^{\mp}$ excitation, respectively.

Theory - Energy shifts and Transition Probabilities

As an example, we obtain for ^{39}K, D_1 line, σ-polarization:

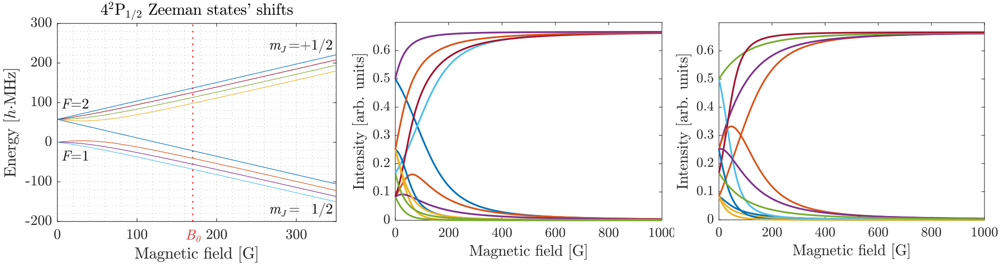

Figure: Left: energy shift of ^{39}K $4^2P_{1/2}$ Zeeman states. Middle and right: A_{eg}/Γ_e of all possible Zeeman transitions as a function of B for $\sigma^{\mp}$ excitation, respectively.

$B_0 = A_{hf}/\mu_B$ ($\sim$ 170 G) is the magnetic field value characterizing establishment of HPB regime. This value is much smaller for K than for Rb or Cs: the range of measurement is increased.

Nanometric thin cell spectroscopy - quick demonstration

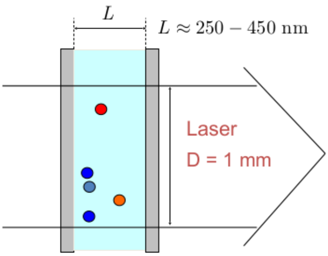

Figure: Scheme of the cell with the laser beam (not to scale).

Nanometric thin cell spectroscopy - quick demonstration

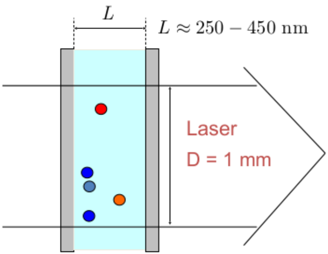

Figure: Scheme of the cell with the laser beam (not to scale).

Time of flight of an atom flying orthogonally to the laser:

$$t_D = \frac{D}{v} = \frac{10^{-3}}{300} \approx \boxed{3\ \mu\text{s}}.$$

Nanometric thin cell spectroscopy - quick demonstration

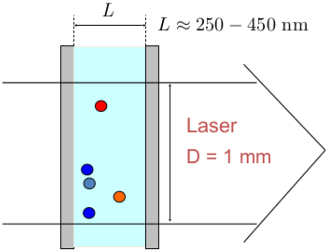

Figure: Scheme of the cell with the laser beam (not to scale).

Time of flight of an atom flying orthogonally to the laser:

$$t_D = \frac{D}{v} = \frac{10^{-3}}{300} \approx \boxed{3\ \mu\text{s}}.$$

Time of flight of an atom flying parallel to the laser:

$$t_L = \frac{L}{v} = \frac{400 \cdot 10^{-9}}{300} \approx \boxed{1.3\ \text{ns}}.$$

Nanometric thin cell spectroscopy - quick demonstration

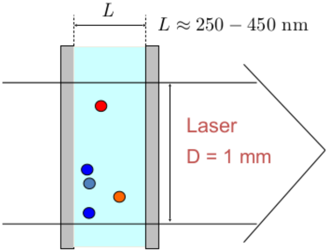

Figure: Scheme of the cell with the laser beam (not to scale).

Time of flight of an atom flying orthogonally to the laser:

$$t_D = \frac{D}{v} = \frac{10^{-3}}{300} \approx \boxed{3\ \mu\text{s}}.$$

Time of flight of an atom flying parallel to the laser:

$$t_L = \frac{L}{v} = \frac{400 \cdot 10^{-9}}{300} \approx \boxed{1.3\ \text{ns}}.$$

Important remark

The geometry of the cell virtually kills all the Doppler broadening! Only atoms flying orthogonally to the laser have time to participate to the signal ($t_L \ll \tau$) but $\mathbf{k} \cdot \mathbf{v} = 0$ for those atoms.

Nanometric thin cell spectroscopy - Absorption spectrum

The cell behaves like a (bad) FP cavity.

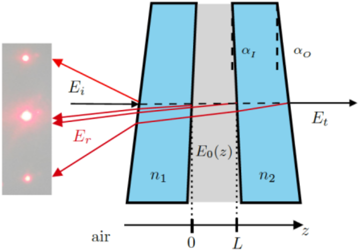

Figure: Scheme of the system with reflected and transmitted beams.

G. Dutier et al. "Revisiting optical spectroscopy in a thin vapor cell: mixing of reflection and transmission as a Fabry–Perot microcavity effect". *J. Opt. Soc. Am. B* **20** (2003), pp. 793–800.

The cell behaves like a (bad) FP cavity.

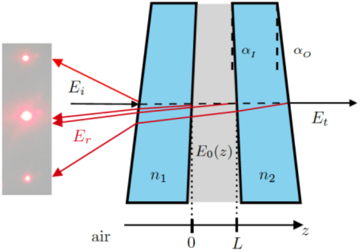

Figure: Scheme of the system with reflected and transmitted beams.

It has been shown that the transmitted and reflected signals read:

$$S_t \approx 2t_{10}t_{02}^2 E_i \Re\left\{I_f - r_1 I_b\right\}/|F|^2\,,$$

G. Dutier et al. “Revisiting optical spectroscopy in a thin vapor cell: mixing of reflection and transmission as a Fabry–Perot microcavity effect”. *J. Opt. Soc. Am. B* **20** (2003), pp. 793–800.

Nanometric thin cell spectroscopy - Absorption spectrum

The cell behaves like a (bad) FP cavity.

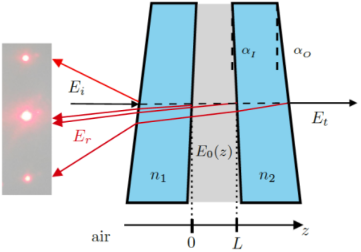

Figure: Scheme of the system with reflected and transmitted beams.

It has been shown that the transmitted and reflected signals read:

$$S_t \approx 2t_{10}t_{02}^2 E_i \Re\left\{I_f - r_1 I_b\right\}/|F|^2 \,,$$

where I_f and I_b are forward and backward integrals of the atomic polarization:

$$I_f = \frac{ik}{2\epsilon_0}\int_0^L P_0(z)\mathrm{d}z$$

$$I_b = \frac{ik}{2\epsilon_0}\int_0^L P_0(z)\exp\left(2ikz\right)\mathrm{d}z\,.$$

G. Dutier et al. "Revisiting optical spectroscopy in a thin vapor cell: mixing of reflection and transmission as a Fabry–Perot microcavity effect". *J. Opt. Soc. Am. B* **20** (2003), pp. 793–800.

Nanometric thin cell spectroscopy - Absorption spectrum

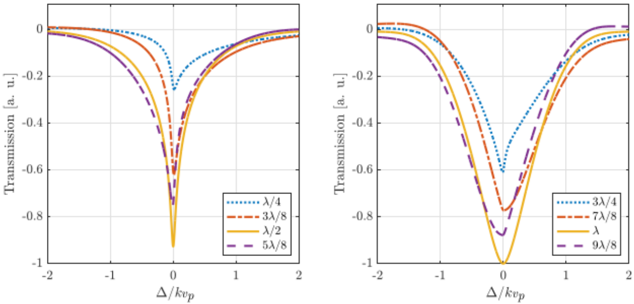

Figure: Theoretical transmission lineshape for two identical sapphire windows ($r_w \approx 0.28$) and $\Gamma/kv_p \approx 0.025$. The thickness varies from $\lambda/4$ to $9\lambda/8$ with a step of $\lambda/8$.

G. Dutier et al. "Revisiting optical spectroscopy in a thin vapor cell: mixing of reflection and transmission as a Fabry–Perot microcavity effect". *J. Opt. Soc. Am. B* **20** (2003), pp. 793–800.

Nanometric thin cell spectroscopy - Absorption spectrum

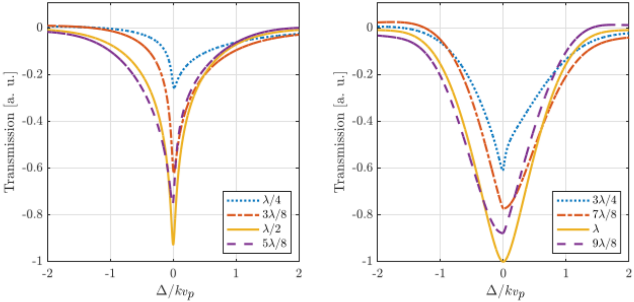

Figure: Theoretical transmission lineshape for two identical sapphire windows ($r_w \approx 0.28$) and $\Gamma/kv_p \approx 0.025$. The thickness varies from $\lambda/4$ to $9\lambda/8$ with a step of $\lambda/8$.

Looping this model over all possible Zeeman transitions allows to obtain sub-Doppler spectra.

G. Dutier et al. "Revisiting optical spectroscopy in a thin vapor cell: mixing of reflection and transmission as a Fabry–Perot microcavity effect". *J. Opt. Soc. Am. B* **20** (2003), pp. 793–800.

Table of Contents

Recently published in Applied Optics

Research Article
Vol. 61, No. 19 / 1 July 2022 / *Applied Optics* 5749

applied optics

Wide range linear magnetometer based on a sub-microsized K vapor cell

M. Auzinsh,[1] A. Sargsyan,[2] A. Tonoyan,[2] C. Leroy,[3] R. Momier,[2,3,*] D. Sarkisyan,[2] and A. Papoyan[2]

[1]*Department of Physics, University of Latvia, Rainis Boulevard 19, LV-1586 Riga, Latvia*
[2]*Institute for Physical Research, NAS of Armenia, Ashtarak-2, 0203, Armenia*
[3]*Laboratoire Interdisciplinaire Carnot de Bourgogne, UMR CNRS 6303, Université Bourgogne Franche-Comté, 21000 Dijon, France*
**Corresponding author: rodolphe.momier@u-bourgogne.fr*

Received 23 March 2022; revised 19 May 2022; accepted 14 June 2022; posted 17 June 2022; published 27 June 2022

^{39}K atoms have the smallest ground state ($^2S_{1/2}$) hyperfine splitting of all the most naturally abundant alkali isotopes and, consequently, the smallest characteristic magnetic field value $B_0 = A_{^2S_{1/2}}/\mu_B \approx 170$ G, where $A_{^2S_{1/2}}$ is the ground state's magnetic dipole interaction constant. In the hyperfine Paschen–Back regime ($B \gg B_0$, where B is the magnitude of the external magnetic field applied on the atoms), only eight Zeeman transitions are visible in the absorption spectrum of the D_1 line of ^{39}K, while the probabilities of the remaining 16 Zeeman transitions tend to zero. In the case of ^{39}K, this behavior is reached already at relatively low magnetic field $B > B_0$. For each circular polarization (σ^-, σ^+), four spectrally resolved atomic transitions having sub-Doppler widths are recorded using a sub-microsized vapor cell of thickness $L = 120-390$ nm. We present a method that allows to measure the magnetic field in the range of $0.1-10$ kG with micrometer spatial resolution, which is relevant in particular for the determination of magnetic fields with large gradients (up to 3 G/µm). The theoretical model describes well the experimental results.

https://doi.org/10.1364/AO.459251

Experimental setup

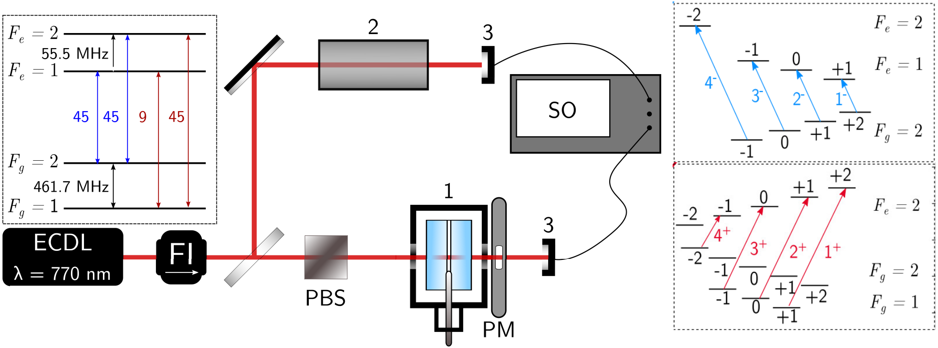

Figure: Experimental setup. Left inset: Hyperfine states of ^{39}K with oscillator strengths. Right inset: Zeeman transition remaining in the HPB regime.

M. Auzinsh et al. "Wide range linear magnetometer based on a sub-microsized K vapor cell". *Appl. Opt.* **61** (2022), pp. 5749–5754.

Results - Spectra

With this simple setup, we track the evolution of the Zeeman transitions while the magnet is brought farther from the cell.

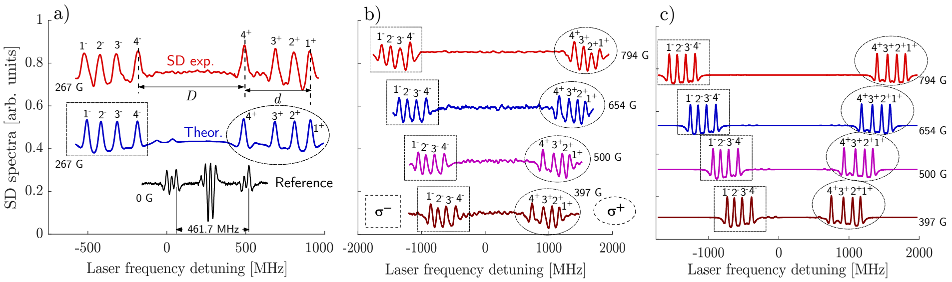

Figure: Theoretical and experimental spectra for $B = 267$ G, $\sigma^{\pm}$ excitation, $L = 385$ nm, $P = 30\ \mu$W.

M. Auzinsh et al. "Wide range linear magnetometer based on a sub-microsized K vapor cell". *Appl. Opt.* **61** (2022), pp. 5749–5754.

Let us compare D and D/d with the theory:

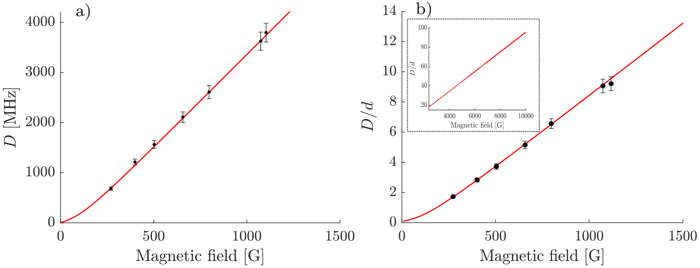

Figure: Frequency distance D between transitions 4^+ and 4^- as a function of B. Solid red line: theory. Dots with error bars: experimental measurements. The inacurracy is around 5%. b) Ratio D/d as a function of B.

M. Auzinsh et al. "Wide range linear magnetometer based on a sub-microsized K vapor cell". *Appl. Opt.* **61** (2022), pp. 5749–5754.

The spectral resolution allows to measures fields with a gradient of up to 3 G/μm.

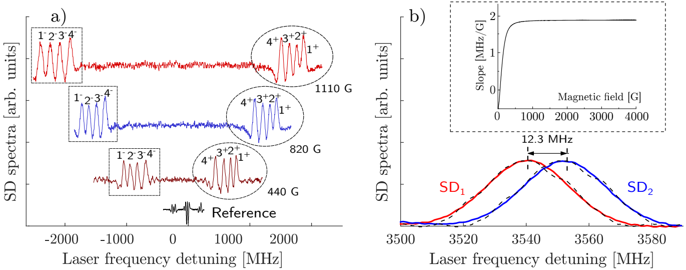

Figure: Spectra recorded for $L = 120 \pm 5$ nm. a) Spectra for B increasing from $B = 440$ to 1110 G. b) Red curve: calculated for $B_1 = 2000$ G, Blue curve: calculated for $B_2 = 2007$ G. Black dashes: experimental measurement obtained by shifting the cell of 2 μm relative to its initial position. This causes a shifts of 12.3 MHz, which is easily measurable.

M. Auzinsh et al. "Wide range linear magnetometer based on a sub-microsized K vapor cell". *Appl. Opt.* **61** (2022), pp. 5749–5754.

Table of Contents

Conclusion

- The small characteristic field value B_0 of ^{39}K makes its convenient to use in atomic magnetometry.

Conclusion

- The small characteristic field value B_0 of ^{39}K makes its convenient to use in atomic magnetometry.
- The thickness of the cell allows to obtain sub-Doppler resolution and track the behavior of the Zeeman transitions.

Conclusion

- The small characteristic field value B_0 of ^{39}K makes its convenient to use in atomic magnetometry.
- The thickness of the cell allows to obtain sub-Doppler resolution and track the behavior of the Zeeman transitions.
- At small cell thickness (120 nm), it becomes possible to measure fields with strong gradient (3 G/μm). Lower thickness will result in line broadening due to atom-atom and atom-surface interactions.

Conclusion

- The small characteristic field value B_0 of ^{39}K makes its convenient to use in atomic magnetometry.
- The thickness of the cell allows to obtain sub-Doppler resolution and track the behavior of the Zeeman transitions.
- At small cell thickness (120 nm), it becomes possible to measure fields with strong gradient (3 G/μm). Lower thickness will result in line broadening due to atom-atom and atom-surface interactions.
- This atomic magnetometry scheme allows to measure a wide range (from 200 G to more than 10 kG) of both uniform and strongly inhomogeneous fields.

Conclusion

- The small characteristic field value B_0 of ^{39}K makes its convenient to use in atomic magnetometry.
- The thickness of the cell allows to obtain sub-Doppler resolution and track the behavior of the Zeeman transitions.
- At small cell thickness (120 nm), it becomes possible to measure fields with strong gradient (3 G/μm). Lower thickness will result in line broadening due to atom-atom and atom-surface interactions.
- This atomic magnetometry scheme allows to measure a wide range (from 200 G to more than 10 kG) of both uniform and strongly inhomogeneous fields.
- Wide range magnetometry is also possible using saturated absorption in a 30 μm cell where cross over resonances are absent. Micrometric cells are much easier to produce than nanocells.

Thank you for your attention.

R. Momier

Dr. A. Sargsyan

Dr. A. Tonoyan

Prof. M. Auzinsh

Prof. D. Sarkisyan

Prof. A. Papoyan

Prof. C. Leroy

Part of the NATO Science for Peace and Security project G5794 team.

References

[1] P. Tremblay et al. "Absorption profiles of alkali-metal D lines in the presence of a static magnetic field". *Phys. Rev. A* **42** (1990), p. 2766.

[2] A. Aleksanyan et al. "Transition cancellations of ^{87}Rb and ^{85}Rb atoms in magnetic field". *J. Opt. Soc. Am. B* **37** (2020), pp. 3504–3514.

[3] E. De Clercq et al. "Laser diode optically pumped caesium beam". *Journal de Physique (France)* **45**.2 (1984), pp. 239–247.

[4] G. Dutier et al. "Revisiting optical spectroscopy in a thin vapor cell: mixing of reflection and transmission as a Fabry–Perot microcavity effect". *J. Opt. Soc. Am. B* **20** (2003), pp. 793–800.

[5] M. Auzinsh et al. "Wide range linear magnetometer based on a sub-microsized K vapor cell". *Appl. Opt.* **61** (2022), pp. 5749–5754.